⌘ *Author's Choice*

THE JOURNAL OF BIOLOGICAL CHEMISTRY VOL. 286, NO. 23, pp. 20375–20386, June 10, 2011

Real-time Analysis of the Inside-out Regulation of Lymphocyte Function-associated Antigen-1 Revealed Similarities to and Differences from Very Late Antigen-4*[S]

Received for publication, November 23, 2010, and in revised form, April 6, 2011 Published, JBC Papers in Press, April 22, 2011, DOI 10.1074/jbc.M110.206185

Alexandre Chigaev[‡1], Yelena Smagley[‡], Yinan Zhang[§], Anna Waller[‡], Mark K. Haynes[‡], Or Amit[‡], Wei Wang[§], Richard S. Larson[‡], and Larry A. Sklar[‡2]

From the [‡]Department of Pathology and Cancer Center and the [§]Department of Chemistry, University of New Mexico Health Sciences Center, Albuquerque, New Mexico 87131

Ten years ago, we introduced a fluorescent probe that shed light on the inside-out regulation of one of the major leukocyte integrins, very late antigen-4 (VLA-4, CD49d/CD29). Here we describe the regulation of another leukocyte integrin, lymphocyte function-associated antigen-1 (LFA-1, CD11a/CD18) using a novel small fluorescent probe in real time on live cells. We found that multiple signaling mechanisms regulate LFA-1 conformation in a manner analogous to VLA-4. LFA-1 can be rapidly activated by Gα_i-coupled G protein-coupled receptors (GPCRs) and deactivated by Gα_s-coupled GPCRs. The effects of Gα_s-coupled GPCR agonists can be reversed in real time by receptor-specific antagonists. The specificity of the fluorescent probe binding has been assessed in a competition assay using the natural LFA-1 ligand ICAM-1 and the LFA-1-specific α I allosteric antagonist BIRT0377. Similar to VLA-4 integrin, modulation of the ligand dissociation rate can be observed for different LFA-1 affinity states. However, we also found a striking difference in the binding of the small fluorescent ligand. In the absence of inside-out activation ligand, binding to LFA-1 is extremely slow, at least 10 times slower than expected for diffusion-limited binding. This implies that an additional structural mechanism prevents ligand binding to inactive LFA-1. We propose that such a mechanism explains the inability of LFA-1 to support cell rolling, where the absence of its rapid engagement by a counterstructure in the inactive state leads to a requirement for a selectin-mediated rolling step.

LFA-1[3] ($\alpha L\beta 2$) and VLA-4 ($\alpha 4\beta 1$) are the two major and, probably, two best studied leukocyte integrins. Together with Mac-1 ($\alpha M\beta 2$, CD11b/CD18, complement receptor 3 (CR3) subunit), they play an important role in the pathogenesis of inflammatory and autoimmune diseases (1, 2). Anti-adhesion therapy is also believed to be a promising concept for the treatment of hematologic malignancies that include malignant lymphoma, acute and chronic leukemias, and others (3–5). A number of LFA-1 and VLA-4 antagonists (antibodies, peptides, and small molecules) have been developed and are undergoing clinical trials (6, 7). Thus, the ability to understand and to regulate VLA-4- and LFA-1-dependent cell adhesion may be critical for the development of successful therapeutic approaches.

In general, integrin-dependent cell adhesion is regulated by rapid conformational changes within the molecule as well as molecular redistribution (clustering), which result from cellular signaling. Numerous proinflammatory immune ligands, chemoattractants, and chemokines can initiate this signaling cascade, often acting through heterotrimeric G proteins (8–11). This, so-called inside-out signaling pathway serves as the basis for rapid cell adhesion and chemotaxis toward sites of inflammation and secondary lymphoid tissues. Rapid integrin activation represents a mechanism for the arrest of rolling leukocytes on the endothelial surface under shear flow (12). Information about the intricate real-time conformational regulation of the VLA-4 integrin and the inside-out signaling pathway was obtained with a fluorescent ligand-mimicking probe (10, 13–17). The goal of these current studies was the development of a fluorescent probe for the assessment of LFA-1 conformational regulation upon triggering of the inside-out signaling pathway.

LFA-1 and VLA-4 exhibit important differences in 1) their expression profile (LFA-1 is exclusively a leukocyte integrin, whereas VLA-4 is also expressed on $CD34^+$ stem cells and nonhematopoietic cells) (1, 18); 2) structural features (LFA-1 contains an additional αA domain (α I domain), where the ligand binding site is localized) (19, 20); 3) different ligand binding motifs and ligands (VLA-4 binds to an alternatively spliced region of fibronectin called the connecting segment 1 (CS-1), VCAM-1, and JAM-2, whereas LFA-1 binds to intercellular adhesion molecules 1–5 (ICAM-1 to -5) and JAM-1) (1, 21);

* This work was supported, in whole or in part, by National Institutes of Health Grants U54 MH084690 and HL081062. This work was also supported by Leukemia and Lymphoma Society Grant 7388-06.

[S] The on-line version of this article (available at http://www.jbc.org) contains supplemental Figs. 1–5.

⌘ *Author's Choice*—Final version full access.

[1] To whom correspondence may be addressed: MSC08 4630, 915 Camino de Salud, Albuquerque, NM 87131. Fax: 505-272-6995. E-mail: achigaev@salud.unm.edu.

[2] To whom correspondence may be addressed: MSC08 4630, 915 Camino de Salud, Albuquerque, NM 87131. Fax: 505-272-6995; E-mail: lsklar@salud.unm.edu.

[3] The abbreviations used are: LFA-1, lymphocyte function-associated antigen-1 (CD11a/CD18, $\alpha L\beta 2$ integrin); fMLFF, *N*-formyl-L-methionyl-L-leucyl-L-phenylalanyl-L-phenylalanine (formyl peptide); FPR, formyl peptide receptor; GPCR, G protein-coupled receptor; ICAM, intercellular adhesion molecule (CD54); JAM, junctional adhesion molecule; MCF, mean channel fluorescence (equivalent of mean fluorescence intensity); PBMC, peripheral blood mononuclear cell; PE, phycoerythrin; VCAM-1, vascular cell adhesion molecule-1 (CD106); VLA-4, very late antigen-4 (CD49d/CD29, $\alpha 4\beta 1$ integrin).

and 4) some well known functional processes (*e.g.* LFA-1 can only support leukocyte firm adhesion (22–24), whereas VLA-4 can support both rolling and firm adhesion) (22, 25–27). Despite these differences, both integrins are implicated as therapeutic targets in diseases, where immunosuppression is envisioned to be beneficial (1, 2). Both VLA-4 and LFA-1 are targeted because of their role in the recruitment of immune cells to an inflamed region. Comparative studies of the two major integrins will provide invaluable information about similarities and differences in the regulation of integrin-dependent cell adhesion. Similarities will identify common signaling pathways that can be modulated upstream of integrin activation. Differences will help our understanding of the specific role of each leukocyte integrin. The current study 1) presents an LFA-1-specific, small fluorescent molecule probe; 2) illustrates the kinetics of probe binding upon triggering of inside-out signaling on live cells in real time; and 3) compares these results with a previously studied VLA-4-specific probe.

EXPERIMENTAL PROCEDURES

Materials—The LFA-1-specific ligands 5-(3-(2-carboxy-2-[2-chloro-4-(3-hydroxy-benzylcarbamoyl)-benzoylamino]-ethyl)-thioureido)-2-(6-hydroxy-3-oxo-3H-xanthen-9-yl)-benzoic acid (compound 1) and 2-[2-chloro-4-(3-hydroxy-benzylcarbamoyl)-benzoylamino]-succinamic acid, (compound 3) (from Refs. 28 and 29) and 5-(4-bromo-benzyl)-3-(3,5-dichlorophenyl)-1,5-dimethyl-imidazolidine-2,4-dione (BIRT0377) (a LFA-1 allosteric antagonist from Ref. 30) were synthesized at the Department of Chemistry and Chemical Biology, University of New Mexico, by Dr. Wei Wang. The VLA-4-specific ligand 4-((*N*′-2-methylphenyl)ureido)-phenylacetyl-L-leucyl-L-aspartyl-L-valyl-L-prolyl-L-alanyl-L-alanyl-L-lysine (LDV) and its FITC-conjugated analog (LDV-FITC probe) (15, 31, 32) were synthesized at Commonwealth Biotechnologies. Mouse anti-human CD11a/LFA-1α, clone HI111 (PE), mouse anti-human fMLP receptor, formyl peptide receptor (FPR) clone 5F1 (PE), mouse anti-human CD184 PE, CXCR4, fusin, clone 12G5 (PE), mouse anti-human CD14 clone M5E2 (PE), and isotype control (mouse IgG1 κ PE) clone MOPC-21 were purchased from BD Biosciences and used according to the instructions of the manufacturer. Human recombinant CXCL12/SDF-1α, recombinant human CXCL8/IL-8, and human recombinant ICAM-1-Fc chimera were from R&D Systems, Inc. Amthamine dihydrobromide (highly selective histamine H2 receptor agonist), tiotidine (histamine H2 receptor antagonist), isoproterenol hydrochloride (selective β-adrenoreceptor agonist), and 118,551-hydrochloride (selective β_2-adrenergic receptor antagonist) were purchased from Tocris Bioscience. Phosphate-buffered saline (PBS) was purchased from Mediatech, Inc. All other reagents were from Sigma-Aldrich. For integrin-specific compounds, stock solutions were prepared in DMSO, at concentrations ~1000-fold higher than the final concentration. Usually, 1 μl of stock solution was added to 1 ml of cell suspension, yielding a final 0.1% DMSO concentration. Control samples were treated with an equal amount of pure DMSO (vehicle). Stock solutions of Gα_s-coupled receptor agonists and antagonists were prepared in water, and control samples were treated with an equal amount of water (vehicle).

Cell Lines and Transfectant Construct—The human histiocytic lymphoma cell line U937 and the human lymphoblastoid cell line JY were purchased from ATCC. Wild type CXCR4 (CD184) receptor-stably transfected U937 cells, wild type CXCR2 (IL8RB)-stably transfected U937 cells, and the non-desensitizing FPR ΔST mutant in U937 cells were prepared as described (33) and were a gift of Dr. Eric Prossnitz (University of New Mexico). High receptor-expressing cells were sorted using a MoFlo flow cytometer (Beckman Coulter). Histamine H2 receptor and β_2-adrenergic receptors are constitutively expressed on U937 cells (34, 35). Cells were grown at 37 °C in a humidified atmosphere of 5% CO_2 and 95% air in RPMI 1640 (supplemented with 2 mM L-glutamine, 100 units/ml penicillin, 100 μg/ml streptomycin, 10 mM HEPES, pH 7.4, and 10% heat-inactivated fetal bovine serum). Cells were harvested and resuspended in 1 ml of HEPES buffer (110 mM NaCl, 10 mM KCl, 10 mM glucose, 1 mM $MgCl_2$, 1.5 mM $CaCl_2$ (or 10 mM $MgCl_2$ and 1 mM EGTA for Mg/EGTA activation experiments) and 50 mM HEPES, pH 7.4) containing 0.1% human serum albumin and stored on ice. The buffer was depleted of lipopolysaccharide by affinity chromatography over polymyxin B-Sepharose (Detoxigel, Pierce). Cells were counted using the Coulter Multisizer/Z2 analyzer (Beckman Coulter). For experiments, cells were suspended in the same HEPES buffer at 1×10^6 cells/ml and warmed to 37 °C. Alternatively, cells were resuspended in warm RPMI (37 °C) and used immediately.

Kinetic Analysis of Binding and Dissociation of LFA-1-specific Ligand—Kinetic analysis of the binding and dissociation of the LFA-1 probe (compound 1) was performed in a manner analogous to the binding of the VLA-4-specific probe described previously (31). Briefly, cells (1×10^6 cells/ml) were preincubated in HEPES buffer containing 0.1% human serum albumin at different conditions for 10–20 min at 37 °C. Flow cytometric data were acquired continuously using a FACScan (BD Biosciences) flow cytometer for up to 1024 s at constant temperature (37 °C) while the samples were stirred continuously at 300 rpm with a 5 × 2-mm magnetic stir bar (Bel-Art Products). Samples were analyzed for 30–120 s to establish a base line. The fluorescent ligand was added, and acquisition was re-established, creating a 5–10-s gap in the time course, which can be observed in the figures. For real-time activation experiments, the LFA-1 probe was added at the concentrations indicated in the figure legends after establishing a base line for unstained cells marked as "autofluorescence." Then data were acquired for 2–3 min, and cells were treated with the indicated GPCR ligands at a receptor-saturating concentration. In several experiments, cells were treated sequentially with two or more compounds. Acquisition was re-established, and data were acquired continuously up to 1024 s.

For kinetic dissociation measurements, cell samples were preincubated with the indicated concentration of LFA-1 probe and treated with GPCR ligands and, as appropriate, excess unlabeled competitor (compound 3, 2 μM). The dissociation of the fluorescent probe was followed. The resulting data were converted to MCF *versus* time using the FCSQuery software developed by Dr. Bruce Edwards (University of New Mexico). Dissociation rate constants (k_{off}) were obtained by fitting dissociation

curves to a single exponential decay equation using GraphPad Prism software (GraphPad Software, Inc.).

GPCR ligand concentrations were chosen based upon known binding affinities (36–41). Ligands were used at concentrations at least 2-fold higher than their respective dissociation constants (K_d). This results in 66% or greater coverage of the receptor sites. For $G\alpha_s$-coupled receptor binding site competition experiments (Fig. 4, *A* and *B*), lower agonist concentrations were chosen to limit potential rebinding after the addition of a large excess of antagonist (20-fold or more). The concentrations of antagonists were chosen based on their respective affinities, to cover more than 99% of the receptor binding sites (200-fold greater than K_d) (36–41). In the absence of $G\alpha_i$-coupled receptor activation, these $G\alpha_s$-coupled receptor agonists and antagonists did not have significant effects upon probe binding.

Estimation of Total LFA-1 (CD11a/LFA-1α) Expression—The expression of CD11a was measured with primary labeled (phycoerythrin) fluorescent mAbs and quantified by comparison with a standard curve generated using Quantum Simply Cellular anti-mouse IgG beads (Bangs Laboratories, Inc.) stained in parallel with the same mAb. This produces an estimate of the total mAb binding sites/cell. Typically, we find 200,000–250,000 LFA-1 sites/JY cell and 90,000–130,000 LFA-1 sites/U937 cell. These numbers were used to estimate maximal binding of the ligand to LFA-1 (*i.e.* B_{max}) in binding curves.

To estimate the effect of inside-out activation upon expression of LFA-1/CD11a, U937 cells were treated with 100 nM fMLFF for 5–10 min at 37 °C under conditions identical to those of the real-time activation experiments. Next, the cells were transferred to ice and stained with anti-CD11a or isotype control antibodies according to the manufacturer's instructions. For histogram analysis, 5000–10,000 events were collected.

Determination of the Relative Fluorescence Quantum Yield—Conjugation (coupling) of fluorophores typically decreases the fluorescence quantum yield. Therefore, to quantify the number of fluorescent molecules bound to the cell surface, we determined the relative quantum yield of the LFA-1 fluorescent probe. Absorption-matched samples of carboxyfluorescein and the fluorescent LFA-1 probe (at 490 nm) were used to acquire emission spectra (supplemental Fig. 1). The relative amount of light transmitted through a 530/30 band pass filter (FL1 channel of the BD FACScan flow cytometer) was ~0.56. This coefficient was used to calibrate the binding of the probe.

Calibration of LFA-1 Probe Binding—The quantum FITC MESF (molecules of equivalent soluble fluorochromes) microsphere kit medium level (Bangs Laboratories, Inc.) was used to quantitate the fluorescence intensity of cells bearing the LFA-1 probe. Drops of beads were added to 0.5 ml of isotonic phosphate-buffered saline (pH 7.2), and the MCF for all calibrated microbeads was collected. The MESF was plotted *versus* the MCF for the four fluorescent microbeads. The graph was used to estimate the total number of molecules of equivalent soluble fluorochromes/cell corresponding to the specific binding of the probe. Next, to calculate MESF values corrected for the differences in the relative quantum yield between fluorescein and LFA-1 probe, values corresponding to LFA-1 probe fluorescence were divided by the coefficient 0.56 (see "Determination of the Relative Fluorescence Quantum Yield"). These MESF values were used to estimate probe dissociation (K_d) constants.

Purification of Human Peripheral Blood Mononuclear Cells (PBMCs)—Human PBMCs were isolated by density gradient centrifugation. Venous blood anticoagulated with heparin or EDTA was obtained from healthy volunteers, and the buffy coat was layered over Ficoll Hypaque (Amersham Biosciences) and centrifuged at 1162 × *g* to obtain mononuclear leukocytes. Leukocytes were washed in DMEM (Invitrogen), resuspended in RPMI 1640 supplemented with 10% heat-inactivated fetal bovine serum, and used immediately. PBMCs were stained using anti-human CD14 PE, anti-human fMLP receptor, anti-human CD184 PE, and isotype control to identify cell subsets according to the manufacturer's instructions.

Statistical Analysis—Curve fits and statistics were performed using GraphPad Prism (GraphPad Software, Inc.). Each experiment was repeated at least three times. The experimental curves represent the mean of two or more independent runs. The S.E. was calculated using GraphPad Prism.

RESULTS

LFA-1-specific Fluorescent Probe—Previously, we developed a VLA-4-specific fluorescent probe based upon BIO 1211 (Biogen, Inc.), a selective VLA-4 antagonist (42, 43). This probe contains LDV, an acidic binding motif, which mimics the prototype LDV ligand within the type III connecting segment of fibronectin and VCAM-1 that employs related, IDS motif sequence (21). Because this molecule represents a competitive antagonist that binds to the same ligand binding site as natural ligands and thus reports the state of the ligand binding pocket, it has been utilized in a number of applications for VLA-4-related studies (10, 13, 15–17, 31, 44, 45).

The vast majority of LFA-1 antagonists are allosteric (6). To develop a probe that reports the state of the ligand binding pocket, it was necessary to identify a direct competitive antagonist for LFA-1. 2-[2-Chloro-4-(3-hydroxy-benzylcarbamoyl)-benzoylamino]-succinamic acid, the compound designed by the transfer of the ICAM-1 three-dimensional epitope to a small molecule (29), was reported to exhibit "classical direct competitive binding behavior with ICAM-1" (28). We proposed to use it as an LFA-1-specific probe (Fig. 1*A*). A non-fluorescent analog was used to determine the nonspecific binding of the probe (Fig. 1*B*). BIRT0377, a highly selective LFA-1-specific α I allosteric antagonist (6, 30) (Fig. 1*C*), was used to assess binding specificity of the LFA-1-specific probe. The evidence that the probe binds to the ICAM-1 binding site is further addressed and substantiated below.

Real-time Binding Kinetics in the Absence of Inside-out Activation Revealed a Slow Step in the Probe Binding—Binding of ligands to LFA-1 requires activation. We were unable to detect any real-time specific binding of the probe in the regular buffer containing 1.5 mM Ca^{2+} plus 1 mM Mg^{2+} or RPMI medium for up to ~700–800 s and concentrations up to ~200 nM (data not shown). This was not surprising because a high concentration of calcium ion is known to be inhibitory for several I-domain-containing integrins (19). A buffer containing $MgCl_2$ and EGTA is usually used for studies of LFA-1-ICAM-1 binding (46,

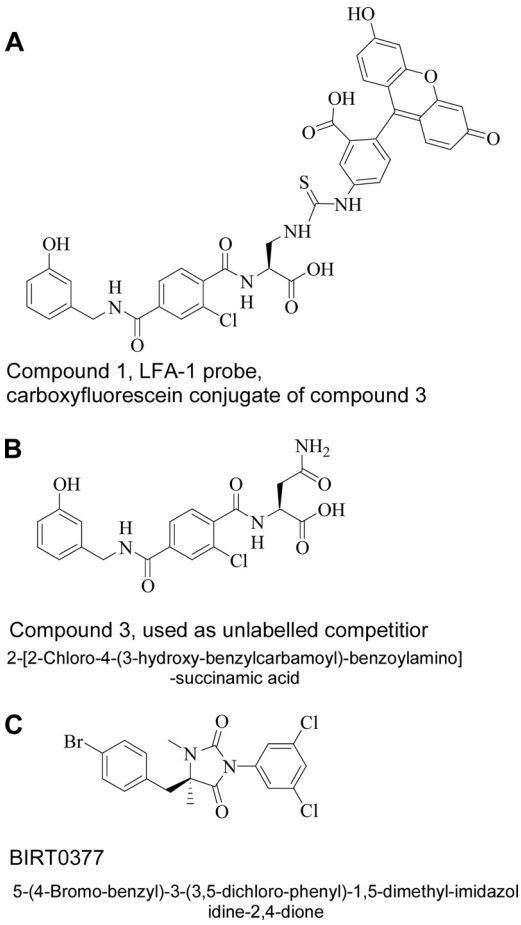

FIGURE 1. **Structures of compounds used in the current study.** *A*, compound 1 (analogous to compound 1 from Ref. 28), LFA-1 probe, a fluorescent analog of compound 3; *B*, compound 3, a non-fluorescent LFA-1-specific probe, used as unlabeled competitor; *C*, BIRT0377, highly selective LFA-1 α I allosteric antagonist (6, 30). All compounds were synthesized at the Department of Chemistry and Chemical Biology, University of New Mexico, by Dr. Wei Wang.

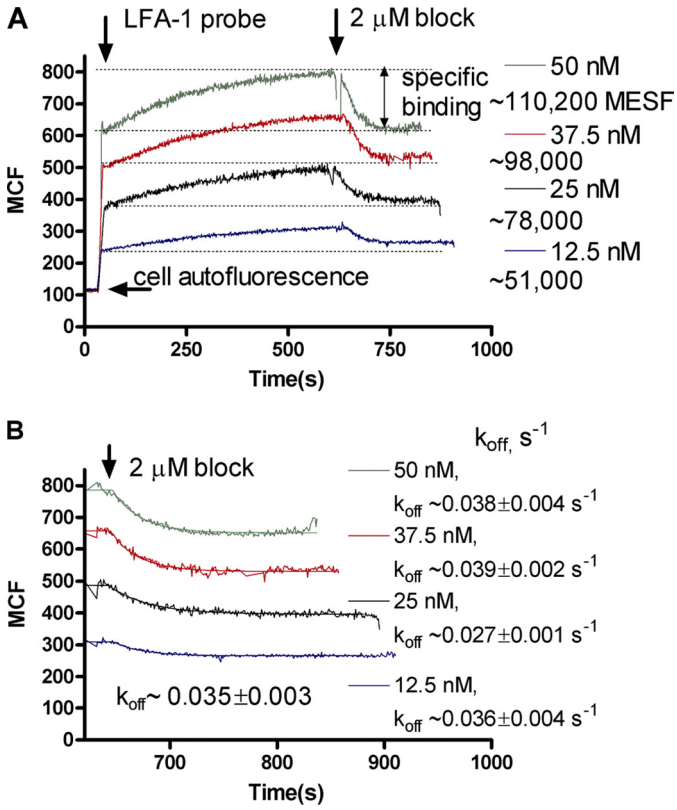

FIGURE 2. **Real-time binding kinetics of the LFA-1 probe (compound 1) in buffer supplemented with Mg^{2+} and EGTA.** *A*, JY cells were consecutively treated with the indicated concentrations of compound 1 (LFA-1 probe), and excess unlabeled competitor (compound 3, 2 μM blocking concentration). The number of LFA-1 sites (MESF), corresponding to the specific binding of the probe, calculated as described under "Experimental Procedures" and in supplemental Fig. 1, is indicated *beside* each curve. Each *line* represents a mean of two independent determinations calculated on a point-by-point basis. The MCF value corresponding to cell autofluorescence is indicated by the *horizontal arrow*. The binding is shown as MCF *versus* time. A representative experiment of five experiments is shown. *B*, a single exponential fit to the dissociation segment of the experimental curves shown in Fig. 2*A* (notice the difference in the *abscissa scale*). Dissociation rates (k_{off} values) are indicated *beside* each curve. The calculated mean ± S.E. k_{off} is shown *under* the experimental curves.

47). Mg^{2+} is known to enhance ICAM-1 binding especially when Ca^{2+} is chelated using EGTA (48). In the presence of Mg^{2+}/EGTA, we observed a very slow but statistically significant real-time accumulation of the probe (Fig. 2*A*). The addition of excess unlabeled probe resulted in rapid probe dissociation (k_{off} ~0.035 ± 0.003 s^{-1} (Fig. 2*B*)). Thus, the slow accumulation of the probe was not related to its uptake or internalization because the probe binding was reversible. It is worth noting that, after the addition of the unlabeled competitor, the probe dissociated to the level corresponding to the nonspecific binding of the probe indicated by *dashed lines* in Fig. 2*A*. The real-time kinetics of nonspecific probe binding is virtually instantaneous, and it also has a linear dependence on concentration; the MCF value doubles as the probe concentration doubles.

Next, using data shown in Fig. 2*A*, we generated an "equilibrium" binding curve. MCF values corresponding to the specific probe binding after equilibrium was reached (shown in Fig. 2*A* by the *vertical double-headed arrow*) were used to estimate MESF according to the calibration line generated using the Quantum FITC MESF kit (medium level), corrected for fluorescence quantum yield (49) as described under "Experimental Procedures." This allowed us to estimate LFA-1 receptor occupancy by the probe at equilibrium. Because the plot did not reach a plateau, in order to estimate the maximal probe binding (B_{max}), we also determined the total number of LFA-1 receptors using anti-CD11a monoclonal antibodies and Quantum Simply Cellular anti-mouse IgG beads (see "Experimental Procedures" for details). This number was found to be ~250,000 sites on JY cells. The fit (supplemental Fig. 2*A*) resulted in a dissociation constant (K_d) of ~60 nM. This number is comparable with the previously reported K_d value for both molecules (compounds 1 and 3, 24 and 95 nM, respectively) in the buffer containing Ca^{2+} and Mg^{2+} (see Table 1 in Ref. 28). To estimate the k_{on} value, we used the dissociation rate obtained in a direct competition (0.036 s^{-1}) (Fig. 2*B*). The calculated k_{on} value was ~6×10^5 M^{-1} s^{-1}.

To estimate the LFA-1 probe association rate using a different approach, curves corresponding to the specific binding of the probe and obtained by subtracting values corresponding to the nonspecific binding from the raw data were fitted to the single phase exponential association equation. Observed *k* val-

ues (k_{obs}, s^{-1}) were plotted *versus* free ligand concentration (supplemental Fig. 2*B*). In this graphical analysis, the slope of the line represents the association rate constant (k_{on}), and the *y* intercept is equal to the ligand dissociation rate (k_{off}). The calculated K_d of ~31 nM was also comparable with the K_d reported for this compound in the buffer containing Ca^{2+} and Mg^{2+} (see Table 1 in Ref. 28).

Rate constants, obtained using this analysis, were significantly slower than expected. The k_{off} value (0.0017 s^{-1}) was ~20 times slower than the k_{off} determined in a direct competitive assay (0.036 s^{-1}) (Fig. 2*B*). The estimated association rate was slower than expected for diffusion-limited binding. For example, for the VLA-4-specific probe (LDV-FITC) that has a higher molecular weight, the k_{on} value is ~3–5 × 10^6 M^{-1} s^{-1} (molecular mass of ~1370 Da) (31). Association rate constant values of ~5–6 × 10^4 M^{-1} s^{-1} are usually reported for large proteins (*e.g.* single-chain variable fragments of antibodies) (50). Moreover, the overall shape of the curves (Fig. 2*A*), consisting of very slow probe association and rapid dissociation, suggested that the binding of the probe is more complex than simple ligand-receptor binding kinetics. Extremely slow binding indicates the presence of a "slow step," which can consist of a receptor conformational change. Identical kinetics (slow probe association with rapid dissociation) was also obtained for U937 cells in buffer supplemented with Mg^{2+}/EGTA. However, because the expression of LFA-1 on U937 cell is about half that of the JY cell, the specific binding signal was significantly lower. Therefore, only data for the JY cell are shown.

Thus, the dissociation of the LFA-1 probe was significantly faster than the approach to equilibrium. One possible interpretation of this phenomenon is that the LFA-1 ligand binding site is shielded by other parts of this or another molecule (*e.g.* in a manner similar to the "endogenous ligand" described in Ref. 51). An additional "slow step" (hypothetically a conformational change resulting in the opening of the ligand binding site) is necessary for ligand binding. Once the ligand is bound, its dissociation is relatively fast. Because the binding of the LFA-1 probe appears to have complex binding kinetics, the rate constants determined in our experiments should be considered as apparent constants. Additional studies are necessary to determine the role of molecular conformation in the regulation of the ligand binding kinetics.

Response Kinetics of LFA-1-specific Fluorescent Probe to Cell Stimulation; Inside-out Activation through Gα$_i$-coupled GPCRs (FPR, CXCR2, and CXCR4)—Integrin affinity and conformation can be rapidly modulated by signaling through G protein-coupled receptors (52), and the majority of receptors involved in leukocyte trafficking and recirculation are pertussis toxin-sensitive Gα$_i$-coupled GPCRs (53). Using the VLA-4-specific probe in our model system, which consists of the monocytic cell line U937 stably transfected with several GPCRs (33), we and others observed rapid receptor-induced affinity changes, rapid molecular unbending (extension), and real-time changes in cellular aggregation and disaggregation (10, 13–16, 31, 44). Here, we employed the same model system to study effects of GPCR signaling on LFA-1 regulation. This is especially feasible because U937 cells were shown to express a significant amount

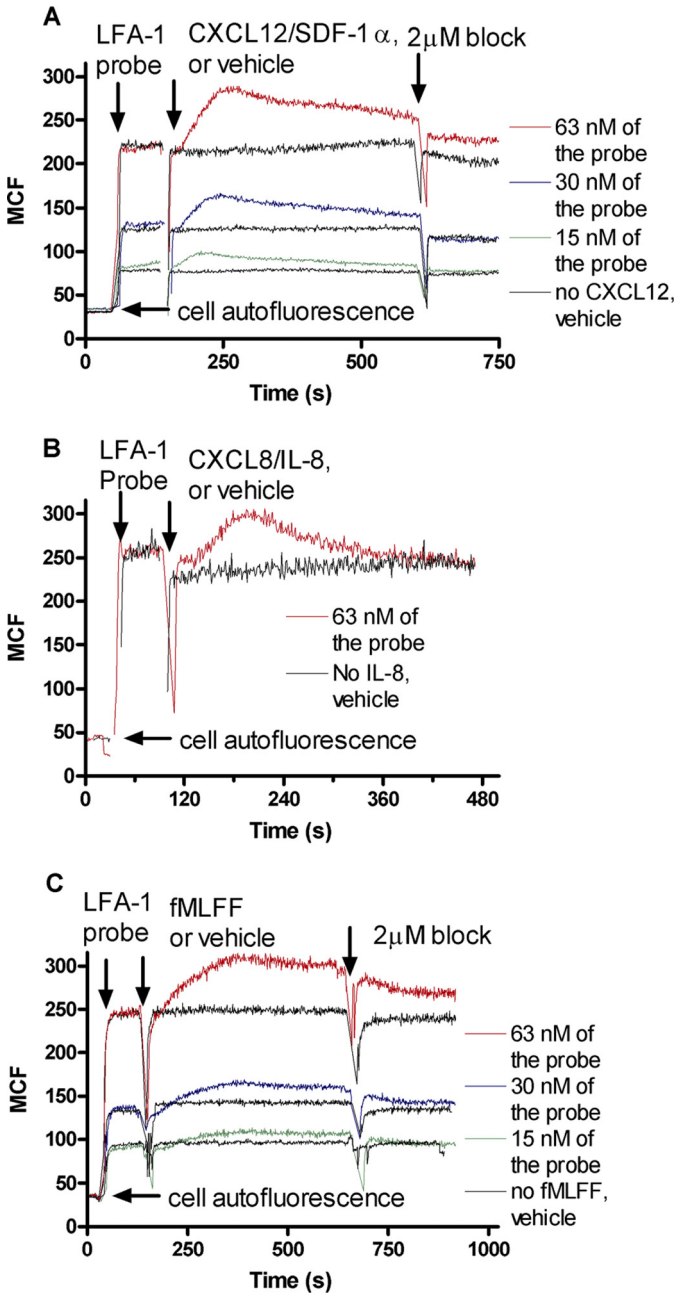

FIGURE 3. **Response kinetics of LFA-1 probe (compound 1) binding following stimulation of CXCR4, CXCR2, and a non-desensitizing mutant of FPR in U937 transfectants.** Cell suspensions were incubated with the indicated concentrations of the LFA-1 probe (compound 1) and stimulated with CXCL12/SDF-1α (*A*), CXCL8/IL-8 (*B*), and fMLFF (*C*). *A*, rapid and transient response of CXCR4-transfected U937 cells to SDF-1. Excess unlabeled competitor (compound 3, 2 μM blocking concentration) was added to determine the nonspecific binding of the probe. *B*, rapid and transient response of CXCR2-transfected U937 cells to IL-8. *C*, rapid and sustained response of FPR ΔST transfectants. Unstimulated control samples (*black lines*) were treated with an equal volume of vehicle (*DMSO*). The MCF value corresponding to cell autofluorescence is indicated by the *horizontal arrow*. The binding of the probe is shown as MCF *versus* time. Each *line* represents the mean of two independent runs calculated on a point-by-point basis. One representative experiment of three experiments is shown.

of LFA-1 and virtually no Mac-1 or (CD11c/CD18, CR4 subunit) αXβ2 integrins (54).

The kinetics of LFA-1 probe binding and dissociation was consistent with the kinetics of previously established receptor signaling for wild type CXCR4 (Fig. 3*A*), wild type IL-8RB

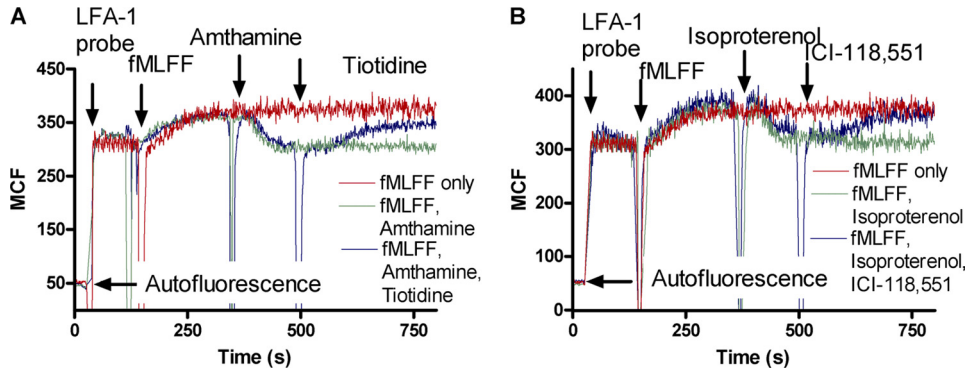

FIGURE 4. **Binding and dissociation of the LFA-1 probe in response to stimulation and inhibition of Gα_s-coupled receptors constitutively expressed on U937 cells.** U937 cells stably transfected with a non-desensitizing mutant of FPR ΔST were sequentially treated with the LFA-1 probe (63 nM), fMLFF (100 nM), and either histamine H2 receptor ligands (amthamine (500 nM), receptor agonist, and tiotidine (10 μM) receptor antagonist) (*A*) or β_2-adrenergic receptor ligands (isoproterenol (1 nM) receptor agonist and ICI-118,551 (10 μM) receptor antagonist) (*B*). *Red lines*, control samples (no Gα_s-coupled receptor ligands were added); *green lines*, samples where only Gα_s-coupled receptor agonists were added; *blue lines*, samples where both Gα_s-coupled receptor agonists and antagonists were added sequentially. The MCF value corresponding to cell autofluorescence is indicated by the *horizontal arrow*. Data are plotted as MCF *versus* time. Each *line* represents the mean of two independent runs calculated on a point-by-point basis. One representative experiment of three experiments is shown.

(CXCR2) (Fig. 3*B*), and a non-desensitizing mutant of formyl peptide receptor (FPR ΔST) (Fig. 3*C*) (55). The probe binding was rapid and reversible for wild type receptors and rapid and sustained after activation of a non-desensitizing GPCR (FPR ΔST). Without activation, the binding of the probe was minimal (see untreated samples; *black lines* in Fig. 3). No slow probe binding, comparable with the kinetics observed for cells treated with Mg^{2+}/EGTA (Fig. 2*A*), was seen in buffer with Ca^{2+}/Mg^{2+}. However, after activation, the binding of the LFA-1 probe was almost as fast as the kinetics of the VLA-4-specific probe (LDV-FITC) (compare Fig. 3 in the current paper with Fig. 4 in Ref 31). This suggests that inside-out signaling facilitates binding of the probe and significantly diminishes the "slow step," which is necessary for ligand binding without inside-out activation.

No Significant Change in CD11a (αL-Integrin Subunit) Expression Was Detected After Inside-out Activation—In order to exclude the possibility that stimulation of Gα_i-coupled receptors rapidly changes surface expression of LFA-1, cells were treated with fMLFF in a manner that was identical to experiments described above (Fig. 3*C*). Next, cells were placed on ice and stained with primary labeled anti-CD11a mAbs and isotype control mAbs (supplemental Fig. 3). The surface expression of CD11a did not change. Thus, Gα_i-coupled receptor signaling had no significant effect upon LFA-1 expression during the time of binding experiments (10–20 min).

Response Kinetics of LFA-1-specific Fluorescent Probe Binding to Gα_s-coupled GPCR (β_2-Adrenergic Receptor, Histamine H2 Receptor) Signaling—Pharmacologic agents that elevate the level of intracellular cAMP down-regulate LFA-1-depedent avidity after T-cell receptor activation (56) and block CXCL8-induced activation of VLA-4 and Mac-1 (12). Ligation of Gα_s-coupled GPCRs, which activates adenylyl cyclase, leads to a rapid down-modulation of VLA-4 affinity after activation through Gα_i-coupled receptors and subsequent cell de-aggregation (17). Therefore, we tested whether the Gα_s-coupled GPCR signaling pathway can modulate the binding of the LFA-1-specific probe.

To study the effect of Gα_s-coupled receptors, we took advantage of two Gα_s-coupled receptors that are constitutively expressed on U937 cells: histamine H2 receptor and β_2-adrenergic receptor (34, 35). The use of a non-desensitizing mutant of FPR allowed us to study the effect of Gα_s-coupled GPCR signaling in real time. Without FPR receptor desensitization, the binding of the LFA-1 probe remained elevated for 1000 s or more (Fig. 4, *red lines*). The addition of specific Gα_s-coupled receptor agonists (amthamine, a histamine H2 receptor agonist (Fig. 4*A*), or isoproterenol, a β_2-adrenergic receptor agonist (Fig. 4*B*)) led to the rapid dissociation of the LFA-1 probe to the level corresponding to the probe binding before cell activation (Fig. 4, *green lines*). Next, to verify that the observed effects are receptor-specific, we used two specific Gα_s-coupled receptor antagonists, tiotidine (histamine H2 receptor antagonist) and ICI-118,551 (β_2-adrenergic receptor antagonist), at concentrations sufficient to block the binding of receptor agonists and, thus, to terminate receptor-mediated signaling (17, 57, 58). The addition of receptor antagonists after cells were treated with Gα_s-coupled receptor agonists completely reversed the suppressive effect of Gα_s-coupled receptor signaling (Fig. 4, *A* and *B*, *blue lines*). At the end of the experiment, the binding of the LFA-1 probe often returned back to the level of the untreated control (Fig. 4, *red lines*, labeled *fMLFF only*). It is worth noting that Gα_s-coupled receptor antagonists by themselves had no effect on fMLFF-activated cells (supplemental Fig. 4); nor did the Gα_s-coupled receptor agonists or antagonists stimulate or inhibit the LFA-1 probe binding when added alone (data not shown). Thus, Gα_s-coupled receptors provide a signal that results in LFA-1 deactivation. This effect is highly receptor-specific because receptor-specific antagonists reversed the effects of Gα_s-coupled receptor agonists. These results were similar to the deactivation kinetics of VLA-4 (compare Fig. 4 with Fig. 2, *A* and *B*, in Ref. 17).

Next, to study LFA-1 regulation on primary peripheral blood leukocytes, we treated PBMCs with forskolin, a specific activator of adenylyl cyclase. Forskolin is known to elevate the concentration of intracellular cyclic adenosine monophosphate in

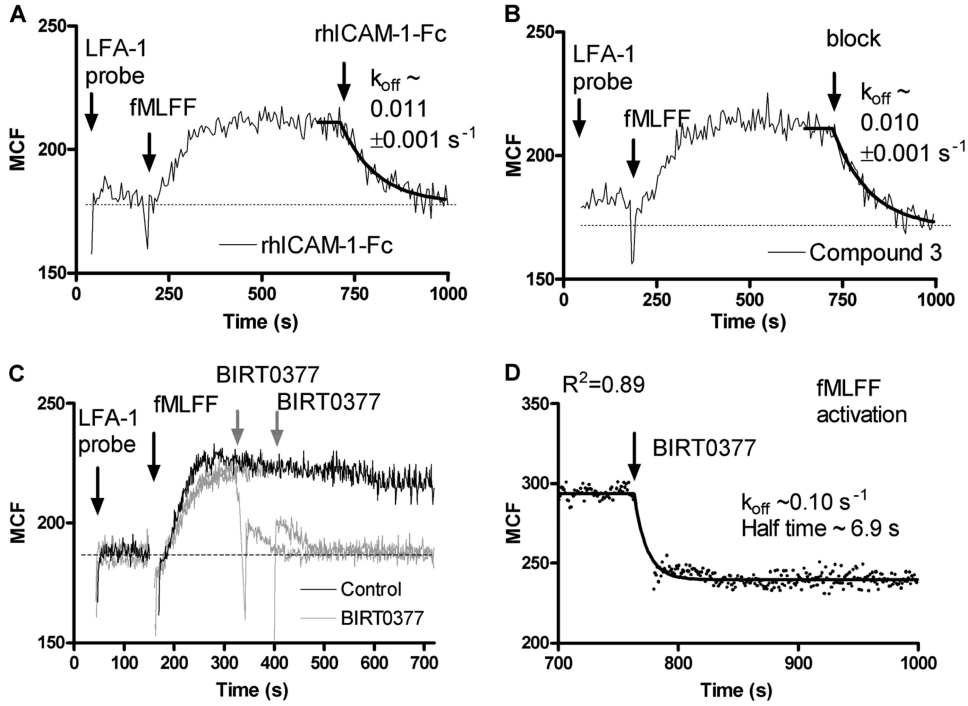

FIGURE 5. **Response kinetics of LFA-1 probe binding to the addition of LFA-1-specific ligands, recombinant human soluble ICAM-1, and LFA-1 allosteric antagonist BIRT0377 (30).** U937 cells stably transfected with the non-desensitizing mutant of FPR ΔST were sequentially treated with the LFA-1 probe (15 nM), fMLFF (100 nM), and human recombinant ICAM-1-Fc chimera (100 nM) (*A*), unlabeled competitor (2 μM block, compound 3) (*B*), or LFA-1-specific allosteric antagonist BIRT0377 (10 μM) (*C* and *D*). Single exponential fits to the dissociation segment of the curves are shown in *A* for ICAM-1, in *B* for compound 3, and in *D* for BIRT0377. Dissociation rates (k_{off} values) are indicated *beside* the curves. Data are plotted as MCF *versus* time. Each *line* represents the mean of two independent runs calculated on a point-by-point basis. One representative experiment of three experiments is shown.

a manner similar to $G\alpha_s$-coupled receptors and thus is considered to mimic signaling through these receptors.

As a result, forskolin significantly diminished binding of the LFA-1 probe to peripheral blood monocytes in response to activation with formyl peptide and to mixed lymphocytes in response to activation using CXCL12 (SDF-1) (supplemental Fig. 5). Thus, the inhibiting effect of cAMP-elevating treatment on inside-out LFA-1 activation can be observed on primary human cells.

Specificity of LFA-1 Probe Binding Assessed Using the Natural LFA-1 Ligand (rhICAM-Fc) and the LFA-1-specific α I Allosteric Antagonist (BIRT0377)—Because the location of the binding site and the mechanism of action of compounds 1 and 3 (28) represent a topic of ongoing interest (see Ref. 59 and references therein), we tested whether the natural LFA-1 ligand (ICAM-1) and α I domain allosteric antagonist (BIRT0377) would affect binding of the LFA-1 probe. Specificity and binding affinity data for the LFA-1 ligand (compound 3) obtained in the equilibrium competition assay using soluble ICAM-1 have been reported previously by Keating *et al.* (28). We used a recombinant human ICAM-1-Fc chimera (R&D Systems, Inc.) as an unlabeled competitor with the LFA-1-specific fluorescent probe to perform real-time kinetic measurements. The addition of excess rhICAM-1-Fc to cells treated with the LFA-1 probe and activated by fMLFF resulted in the dissociation of compound 1 (Fig. 5*A*). The dissociation rates obtained using rhICAM-1-Fc and excess unlabeled competitor (compound 3, block) were identical (k_{off} = 0.011 ± 0.001 s^{-1} and 0.010 ± 0.001 s^{-1}) (Fig. 5, *A* and *B*). Because an unlabeled competitor prevents rebinding of the fluorescent probe simply by binding to the same ligand binding site, an exponential decrease in cell fluorescence reflects the dissociation of the fluorescent probe. This suggests that rhICAM-Fc competes directly with the LFA-1 probe (compound 1). Thus, real-time competition of unlabeled soluble human ICAM-1 with the fluorescent probe further supports the idea that compound 1 is a direct LFA-1 antagonist (28, 59).

Next, we used BIRT0377 (Fig. 1*C*), an LFA-1-specific α I allosteric antagonist (6, 30, 60), to probe its effect on binding of compound 1. The addition of BIRT0377 to the ΔST FPR-expressing cells, pretreated with the LFA-1 probe and activated by fMLFF, induced rapid dissociation of the probe (k_{off} ~0.1 s^{-1}) (Fig. 1*D*). The rate of probe dissociation in this case was ~10 times faster than the k_{off} induced by excess unlabeled competitor (Fig. 5*B*) or natural LFA-1 ligand (Fig. 5*A*). This suggests that the binding of BIRT0377 by itself (no unlabeled competitor was added) triggers dissociation of the probe by lowering the affinity of the ligand binding pocket. Faster ligand dissociation rates (k_{off} values) correspond to the states of lower affinity for at least one previously studied integrin fluorescent probe (LDV-FITC) (17, 31). Recently discovered allosteric antagonists of VLA-4 integrin also induce rapid probe dissociation (61). Thus, these data are in agreement with the observation that α I allosteric antagonists stabilize a low affinity conformation of the α I domain (6, 62). It is worth noting that the addition of BIRT0377 caused probe dissociation to a level similar to the level of binding before cell activation (see the base line in Fig. 5*C*). The probe dissociation rate was also similar to the k_{off} for resting cells (Table 1). Taken together, these results suggest that the conformational state induced by BIRT0377 is quantitatively similar to the LFA-1 resting state. It has been reported

TABLE 1

Summary of LFA-1 probe (compound 1) dissociation rates for different activation states of LFA-1 induced using different LFA-1-specific ligands and antagonists

Cell treatment (activation)	k_{off}[a]
	s^{-1}
Resting state, in buffer supplemented with Ca^{2+} and Mg^{2+}, induced by the addition of compound 3 after reversible activation through CXCR4 (see Fig. 7, *A* and *B*)	0.180 ± 0.092
Activated through a non-desensitizing mutant of FPR, induced by the addition of compound 3 (see Fig. 5*B*)[b]	0.015 ± 0.006
Activated through a non-desensitizing mutant of FPR, induced by the addition of BIRT0377 (see Fig. 5*C, D*)[c]	0.100 ± 0.020
Activated through a non-desensitizing mutant of FPR, induced by the addition of rhICAM-1-Fc (see Fig. 5*A*)	0.011 ± 0.009

[a] Rates were determined using the single exponential fit equation and GraphPad Prism software. Mean ± S.E. from 2–3 independent experiments performed on different days are shown.

[b] After receptor ligation, wild type GPCRs are rapidly desensitized and internalized, making it difficult to estimate integrin ligand dissociation rates (see Fig. 3, *A* and *B*). The ΔST FPR mutant lacks all of the potential serine or threonine phosphorylation sites in the carboxyl terminus, and it has been shown to mediate a sustained ligand-induced signaling without ligand-induced internalization or desensitization (80, 81). It remains in the signaling conformation for 1000 s or longer, allowing the determination of ligand dissociation rates for the activated integrin state (see Figs. 3*C* and 5 (*A* and *B*)).

[c] Formally, the rate of probe dissociation induced by the addition of BIRT0377 does not represent the probe dissociation rate. It is composed of the rate of the BIRT0377 binding, the rate of the BIRT0377-induced conformational change, and the rate of the probe dissociation as a result of this conformational change. However, it can be considered a lower limit of k_{off}.

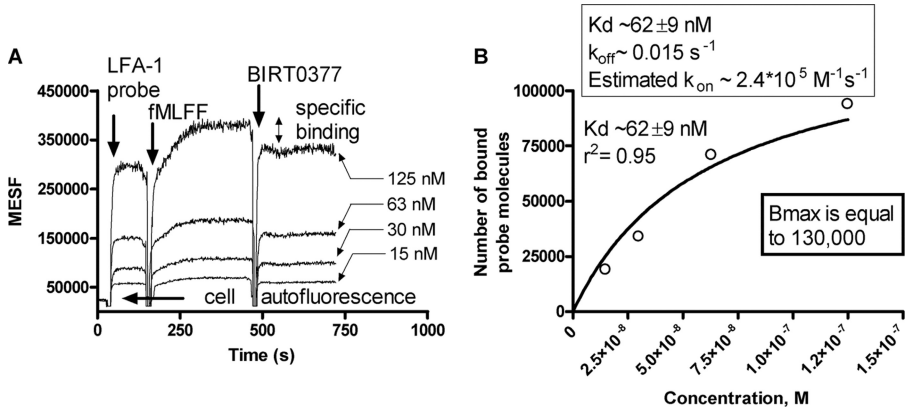

FIGURE 6. **Determination of LFA-1 probe binding affinity for cells activated by sustained $G\alpha_i$-coupled GPCR signaling using real-time binding kinetics of the LFA-1 probe (compound 1) in buffer supplemented with Mg^{2+} and Ca^{2+}.** *A*, U937 cells stably transfected with the non-desensitizing mutant FPR ΔST were consecutively treated with the indicated concentrations of the LFA-1 probe (compound 1), fMLFF (100 nM), and LFA-1-specific allosteric antagonist BIRT0377 (10 μM) to determine specific binding of the probe. Each *line* represents the mean of two independent runs calculated on a point-by-point basis. The binding is shown as MESF *versus* time. The number of LFA-1 sites (MESF), corresponding to the specific binding of the probe, is calculated as described under "Experimental Procedures" and in supplemental Fig. 1. The MESF value corresponding to cell autofluorescence is indicated by the *horizontal arrow*. A representative experiment of three experiments is shown. *B*, equilibrium binding curve generated using experimental data shown in Fig. 6*A*. The number of LFA-1 sites (MESF) corresponding to specific binding of the probe was plotted *versus* free probe concentration. Because the overall concentration of LFA-1 is less than 0.3 nM (~130,000 CD11a sites/U937 cell (estimated as described under "Experimental Procedures"); 10^6 cells/ml results in ~0.27 nM), no significant ligand depletion is expected. Because the curve did not reach a plateau, the maximal probe binding was constrained to 130,000 (the total number of LFA-1s/U937 cell). The on-rate (k_{on}) was estimated as the ratio k_{off}/K_d.

that the effect of BIRT0377 on LFA-1-mediated events is highly selective, that it has no effect on Mac-1/ICAM-1- or VLA-4-mediated events (30), and that BIRT0377 specifically binds to LFA-1 α I-domain (6, 60) containing the ICAM-1 binding site. In combination, these data support the idea that the LFA-1 probe (compound 1) is highly selective and can be used as an artificial LFA-1 ligand reporting the state of the LFA-1 binding pocket. This conclusion is especially notable in light of the technique that was employed to design this molecule, namely by a transfer of the ICAM-1 binding epitope to a small molecule (29).

Additionally, we tested whether binding of the LFA-1 probe can be blocked by a VLA-4-specific, LDV-containing small molecule (unlabeled) previously used to detect changes in the VLA-4 affinity and conformation and, vice versa, whether the binding of VLA-4 probe (LDV-FITC) can be blocked by compound 3 (LFA-1 probe, unlabeled competitor) (13, 16, 17). As expected, no significant competition was observed (data not shown). Thus, binding of the LFA-1 probe is specific because it can be blocked by a natural LFA-1 ligand (soluble human ICAM-1) or by an LFA-1-specific α I allosteric antagonist (BIRT0377) but not by VLA-4-specific ligands.

Binding Affinity of the LFA-1 Probe after Inside-out Activation—To estimate the probe binding affinity after inside-out activation, we used an experimental approach described in supplemental Fig. 2. Cells expressing a non-desensitizing mutant of FPR were treated with different concentrations of the probe and activated using fMLFF (Fig. 6*A*). To determine the MCF value corresponding to the specific binding for each probe concentration, BIRT0377 was added after equilibrium was reached. Because the plot did not reach a plateau, the maximal probe binding (B_{max}) was also estimated based on LFA-1 expression on U937 cells, which was determined using anti-CD11a monoclonal antibodies and Quantum Simply Cellular anti-mouse IgG beads as described above. On U937 cells this number was found to be ~130,000 sites, and therefore, the B_{max} for the fit (Fig. 6*B*) was constrained to 130,000. The dissociation constant (K_d) was ~62 nM. This number is similar to a K_d value for the binding of the probe in Mg^{2+}/EGTA-containing buffer (supplemental Fig. 2*A*). To estimate the k_{on}, we used the value

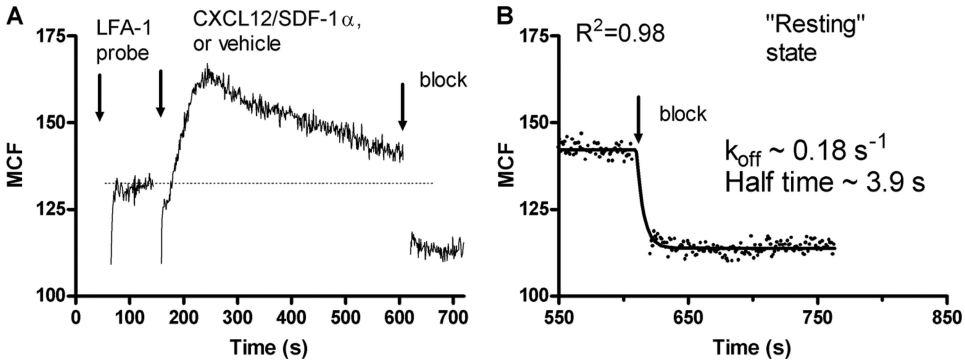

FIGURE 7. **Determination of the LFA-1 probe dissociation rate on "resting" U937 cells in the buffer supplemented with Mg^{2+} and Ca^{2+} using the rapidly desensitizing wild type CXCR4 receptor.** *A*, U937 cells stably transfected with the wild type CXCR4 receptor were consecutively treated with the LFA-1 probe (30 nM, compound 1), fMLFF (100 nM), and excess unlabeled competitor (compound 3; 2 μM blocking concentration). *B*, the dissociation segment of the curve was fitted to a single exponential equation. The dissociation rate (k_{off}) is shown *beside* the curve. The binding is shown as MCF *versus* time. Each *line* represents the mean of two independent runs calculated on a point-by-point basis. One representative experiment of three experiments is shown.

of the dissociation rate obtained in a direct competition assay (the average from multiple experiments was $\sim$0.015 s^{-1}) (Fig. 5*B*). The calculated k_{on} value was $\sim 2.4 \times 10^5$ M^{-1} s^{-1}.

The analysis of the probe binding affinity after sustained inside-out activation revealed similar binding constants compared with the activated state induced in the Mg^{2+}/EGTA-containing buffer. The K_d and k_{off} values are only 2-fold different. Therefore, calculated k_{on} values are also similar. However, the probe real-time binding kinetics appears dramatically different (compare Fig. 2*A* and Fig. 3*C* or 5 (*A*–*C*)). In the Mg^{2+}/EGTA buffer, the approach to equilibrium takes $\sim$600 s or more (half-time $\sim$200–300 s), whereas in the Ca^{2+}/Mg^{2+} buffer, after $G\alpha_i$ receptor ligation, it requires less than 100 s (half-time $\sim$30–40 s). We postulate that this difference is caused by significantly different integrin conformations. Determination of the resting dissociation constant (K_d) in the Ca^{2+}/Mg^{2+} buffer, which is close to normal physiological conditions, using our tools was not possible because of the lack of significant specific binding in the absence of inside-out activation (see Fig. 3, *black lines*).

LFA-1 Activation Results in the Modulation of the Ligand Dissociation Rate—The VLA-4 integrin exhibits multiple affinity states, which can be detected in real time using ligand dissociation rate analysis (31, 32, 42). Therefore, we specifically focused on the analysis of the LFA-1 probe dissociation rates at rest and upon activation. The binding of the LFA-1 probe to the receptor in the absence of inside-out activation in a buffer containing Ca^{2+} and Mg^{2+} is very small (see Fig. 3). Therefore, to obtain an estimate of the dissociation rate for the resting LFA-1 receptor, we took advantage of a rapidly desensitizing wild type GPCR. Cells expressing wild type CXCR4 were treated consecutively with LFA-1 probe and CXCL12 (Fig. 7*A*). This resulted in rapid probe binding followed by spontaneous probe dissociation due to receptor desensitization. Excess unlabeled competitor was added close to the time when the binding of the probe returned to the level corresponding to the base line, before the addition of CXCL12. The dissociation rate determined at this moment should be considered a lower estimate (Fig. 7*B*). The "actual" resting k_{off} should be faster because of the small number of integrin receptors in the active conformation that are still present on the cell surface at this time. Activation through a constitutively active ΔST FPR mutant results in 5–8-fold slower dissociation rates (Table 1). The difference in the probe k_{off} for the resting *versus* activated cells is comparable with the relative change in the dissociation rates for a VLA-4-specific (LDV-FITC) probe on inside-out activation (31). This suggests a quantitatively similar ability of the inside-out signaling pathway to modulate ligand dissociation rates of the integrin ligand binding pocket for two different integrins. Cell treatment with BIRT0377 resulted in a k_{off} similar to the resting state of the LFA-1 on U937 cells. This result is not surprising because BIRT0377 is known to stabilize the low affinity conformation of LFA-1 α I domain (6, 62). Taken together, our data suggest that the LFA-1 probe dissociation rate is regulated in a manner similar to the rate for the other leukocyte integrin, VLA-4.

DISCUSSION

The idea that a fluorescent small molecule, which specifically binds to an integrin ligand binding site, can be used for real-time detection of rapid conformational changes of the integrin ligand-binding pocket on live cells is not novel. Previously, we used a low molecular weight ligand-mimicking fluorescent probe to study the conformational regulation of VLA-4, a non-α I domain containing leukocyte integrin (15, 16, 31, 32, 44, 63). One advantage of this approach is that, because of its size, small molecule binding is rapid and sensitive to integrin affinity changes. For example, compare LFA-1 probe binding here with the binding of soluble recombinant ICAM-1 (64). This allows the detection of short lived and transient changes in ligand binding in singlet cell populations regardless of cell-cell interactions. Because of the ability of a regular flow cytometer to discriminate between free and bound fluorescent ligand in solution, these experiments are performed as a homogeneous assay by simply adding multiple ligands to a live cell suspension. The continuous sampling before, during, and after receptor signaling provides unique information about real-time signaling kinetics. The current work presents data acquired using the same well characterized model system, which consists of U937 cells stably transfected with different GPCRs, to study the real-time conformational regulation of LFA-1. A comparison of the real-time binding kinetics of VLA-4- and LFA-1-specific probes revealed multiple similarities and a difference.

In a manner similar to VLA-4, multiple signaling mechanisms are capable of regulating LFA-1: 1) activation through $G\alpha_i$-coupled GPCR (CXCR4, FPR1, and CXCR2) signaling pathways with the kinetics of activation dependent upon receptor desensitization; 2) LFA-1 deactivation upon ligation of $G\alpha_s$-coupled GPCRs (HRH2 and ADRB2), which can be reversed in real time by the receptor-specific antagonists; 3) modulation of the ligand dissociation rate after the inside-out signal. All of these are not surprising, considering an evolutionary similarity between these two major leukocyte integrins. According to a phylogenetic tree, the α_4-integrin subunit is most closely related to the I-domain-containing integrin subunit cluster that includes αL (see Fig. 2 in Ref. 65). This suggests that the majority of inside-out activation and deactivation mechanisms would be preserved because leukocyte-specific, α I domain-containing integrin subunits (αD, αE, αL, αM, and αX) appear after non-α I domain-containing integrins (66). However, there is a well documented physiological difference between the two molecules. VLA-4 is a "variable capture receptor." It can support both rolling and firm adhesion (22, 25–27). LFA-1 is predominantly a firm attachment receptor, and therefore, it requires selectins for the rolling step prior to activation and adhesion (22–24).

Our data suggest that in the absence of inside-out activation, binding of a small ligand to LFA-1 is extremely slow. In contrast, binding of a small molecule ligand (LDV-FITC) to VLA-4 is fast, and the LDV-FITC association rate (k_{on}) is largely independent of the integrin activation state (see Table 2 in Ref. 32). This implies that an additional structural mechanism prevents ligand binding to inactive LFA-1. Such a "protective mechanism" could explain 1) the absence of LFA-1 engagement by its counterstructure (ICAM-1 and others) in the inactive (resting) state; 2) its inability to support cell rolling; and thus 3) a requirement for a selectin-mediated rolling step.

It is postulated that the kinetics of "bond" formation and dissociation is critical for adhesive interactions. The rapid on-rate is specifically important for cell rolling, because a fast interaction is required between rapidly flowing cells and a substrate (24). Our present data indicate that the on-rates for the binding of a small ligand to VLA-4 and LFA-1 are dramatically different. The on-rate for the small ligand binding to VLA-4 is close to the diffusion-limited rate for a small ligand of this size (32). For the LFA-1-specific probe, this rate is at least 10 times slower. This explains the inability of LFA-1 to support tethering and rolling. Notably, the possibility of such a difference was predicted by Alon *et al.* in 1995 (see "Discussion" in Ref. 25).

It is tempting to attribute the difference in ligand binding to a major structural difference between VLA-4 and LFA-1 because LFA-1 has an additional "inserted" α I domain (αA domain), which contains the ICAM-1 binding site. "Shielding" of the ligand binding site by a part of the molecule would be an ideal mechanism to explain this difference (*e.g.* a mechanism similar (but not identical) to an "endogenous ligand" described by Alonso *et al.* (51) that blocks the α/β I-like allosteric antagonist binding site). The putative ligand binding site "protection" can be rapidly released through a well documented large conformational rearrangement (*e.g.* unbending or extension) of LFA-1 upon activation (67), which results in rapid binding of the ligand. Without inside-out activation, extension of the LFA-1 molecule can be induced by XVA143, an α/β I-like allosteric antagonist. Because binding of XVA143 does not up-regulate LFA-1 affinity, the XVA143-induced conformational change supports rolling on ICAM-1 (68), presumably through a release of the LFA-1 ligand binding site "protection." We hypothesize that this mechanism requires expression of the whole LFA-1 molecule, because when isolated and immobilized on particles, the I-domain, by itself, is capable of mediating capture and rolling on ICAM-1-coated surfaces under shear flow in a manner very similar to selectin-carbohydrate interactions (69).

Integrin Antagonists, Direct (Competitive) Versus Allosteric—Another remarkable difference between integrins lies within the type of small molecules, developed and reported to modulate integrin dependent cell adhesion, small integrin antagonists. The majority of αIIbβ3, αvβ3, and α4β1 integrin-specific small molecule ligands are competitive antagonists. In contrast, LFA-1 (αLβ2) integrin-specific small molecules are mostly allosteric antagonists (6, 70). Is there a specific reason for this distinction? The data presented here suggest a plausible explanation for this phenomenon.

Competitive antagonists would be inefficient in blocking LFA-1-dependent cell adhesion if on resting cells the LFA-1 binding domain is "hidden" and only exposed after inside-out activation. A competitive LFA-1 antagonist would not bind to the cell surface prior to activation, and therefore, only after activation would it compete in real time with a natural integrin ligand. There could be especially inefficient competition at sites, where immobilized chemokines and natural integrin ligands coexist in proximity on the surface of endothelia (12, 67, 71). Therefore, allosteric antagonists, with unobstructed binding to sites distinct from the ligand binding pocket, could efficiently stabilize the inactive (resting) integrin conformation (*e.g.* see Ref. 72 for BIRT0377 data). Allosteric antagonists could be the most efficient way to prevent cell adhesion for those integrins with a hidden ligand binding site in the resting state. As a result, in screening assays aimed at identifying LFA-1 antagonists, the number of allosteric "hits" should be artificially enriched. Thus, taken together, these ideas suggest two suitable approaches to identify competitive LFA-1 antagonists. These would include 1) analysis of the structure of the ICAM-1/LFA-1 binding epitope as in the design of compounds 1 and 3 (28, 29) used in the current paper or 2) the use of these compounds with activated LFA-1 in high throughput screens.

Integrin Deactivation and Cell Deadhesion—Historically, the major focus of cell adhesion studies was on leukocyte receptors that up-regulate cell adhesion and stimulate cell migration. The majority of chemotactic receptors in hematopoietic cells are $G\alpha_{i/o}$-coupled GPCRs (73, 74). However, recent reports suggest that in addition to $G\alpha_{i/o}$-coupled GPCR-triggered activation, inactivating signaling pathways that trigger down-regulation of integrin affinity can play a role in modulation of immune cell adhesion and cell mobilization. The $G\alpha_s$-coupled GPCR/cAMP-dependent pathway actively down-modulates VLA-4 activation and thus induces cellular disaggregation (17). Presumably, this type of signaling provides a mechanism for stress-induced leukocytosis (75–77) and results in the mobi-

lization of multiple leukocyte subsets that include $CCR7^{-}CD45RA^{+}CD8^{+}$ effector T cells, $CD4^{-}CD8^{-}$ γ/δ T cells, $CD3^{+}CD56^{+}$ NKT-like cells, $CD16^{+}$CD56dim cytotoxic NK cells, and CD14dim$CD16^{+}$ proinflammatory monocytes, all with a cytotoxic effector function that defines a first line of immunological defense (78, 79).

Data presented here suggest that LFA-1 can be inactivated by $G\alpha_s$-coupled GPCR/cAMP-dependent signaling in a manner similar to VLA-4. This implies that LFA-1-dependent immune cell-cell interactions that include interaction of immune cells with antigen-presenting cells, T- and B-cell interactions, and others can be directly affected by inside-out integrin deactivation. This can shift the focus of future research from studies of integrins and innate immunity mechanisms (usually related to VLA-4) toward the regulation of adaptive immune responses that are dependent on antigen-specific cell-cell interaction supported by LFA-1. Moreover, our recent data suggest that in addition to the $G\alpha_s$-coupled GPCR/cAMP-dependent pathway, other signaling pathways can actively down-modulate integrin activation.[4] This creates additional diversity in the network of immune cell signaling and interactions.

Acknowledgments—We thank Eric R. Prossnitz for providing U937 cells and plasmids and Bruce S. Edwards for providing FCSQuery software. We thank Gregory C. Davenport, Prakasha Kempaiah, and Douglas J. Perkins for help with PBMC preparation.

REFERENCES

1. Hyun, Y. M., Lefort, C. T., and Kim, M. (2009) *Immunol. Res.* **45,** 195–208
2. Yusuf-Makagiansar, H., Anderson, M. E., Yakovleva, T. V., Murray, J. S., and Siahaan, T. J. (2002) *Med. Res. Rev.* **22,** 146–167
3. Schmidmaier, R., and Baumann, P. (2008) *Curr. Med. Chem.* **15,** 978–990
4. Matsunaga, T., Takemoto, N., Sato, T., Takimoto, R., Tanaka, I., Fujimi, A., Akiyama, T., Kuroda, H., Kawano, Y., Kobune, M., Kato, J., Hirayama, Y., Sakamaki, S., Kohda, K., Miyake, K., and Niitsu, Y. (2003) *Nat. Med.* **9,** 1158–1165
5. Matsunaga, T., Fukai, F., Miura, S., Nakane, Y., Owaki, T., Kodama, H., Tanaka, M., Nagaya, T., Takimoto, R., Takayama, T., and Niitsu, Y. (2008) *Leukemia* **22,** 353–360
6. Shimaoka, M., and Springer, T. A. (2003) *Nat. Rev. Drug Discov.* **2,** 703–716
7. Cox, D., Brennan, M., and Moran, N. (2010) *Nat. Rev. Drug Discov.* **9,** 804–820
8. Alon, R., and Feigelson, S. W. (2009) *Microcirculation* **16,** 3–16
9. Laudanna, C., Kim, J. Y., Constantin, G., and Butcher, E. (2002) *Immunol. Rev.* **186,** 37–46
10. Hyduk, S. J., and Cybulsky, M. I. (2009) *Microcirculation* **16,** 17–30
11. Zarbock, A., and Ley, K. (2009) *Microcirculation* **16,** 31–42
12. Laudanna, C., and Alon, R. (2006) *Thromb. Haemost.* **95,** 5–11
13. Chigaev, A., Waller, A., Zwartz, G. J., Buranda, T., and Sklar, L. A. (2007) *J. Immunol.* **178,** 6828–6839
14. Hyduk, S. J., Chan, J. R., Duffy, S. T., Chen, M., Peterson, M. D., Waddell, T. K., Digby, G. C., Szaszi, K., Kapus, A., and Cybulsky, M. I. (2007) *Blood* **109,** 176–184
15. Chigaev, A., Buranda, T., Dwyer, D. C., Prossnitz, E. R., and Sklar, L. A. (2003) *Biophys. J.* **85,** 3951–3962
16. Chigaev, A., Waller, A., Amit, O., Halip, L., Bologa, C. G., and Sklar, L. A. (2009) *J. Biol. Chem.* **284,** 14337–14346
17. Chigaev, A., Waller, A., Amit, O., and Sklar, L. A. (2008) *BMC Immunol.* **9,** 26
18. Lapidot, T., Dar, A., and Kollet, O. (2005) *Blood* **106,** 1901–1910
19. Shimaoka, M., Takagi, J., and Springer, T. A. (2002) *Annu. Rev. Biophys. Biomol. Struct.* **31,** 485–516
20. Arnaout, M. A., Mahalingam, B., and Xiong, J. P. (2005) *Annu. Rev. Cell Dev. Biol.* **21,** 381–410
21. Humphries, J. D., Byron, A., and Humphries, M. J. (2006) *J. Cell Sci.* **119,** 3901–3903
22. Fabbri, M., Bianchi, E., Fumagalli, L., and Pardi, R. (1999) *Inflamm. Res.* **48,** 239–246
23. von Andrian, U. H., Chambers, J. D., McEvoy, L. M., Bargatze, R. F., Arfors, K. E., and Butcher, E. C. (1991) *Proc. Natl. Acad. Sci. U.S.A.* **88,** 7538–7542
24. Lawrence, M. B., and Springer, T. A. (1991) *Cell* **65,** 859–873
25. Alon, R., Kassner, P. D., Carr, M. W., Finger, E. B., Hemler, M. E., and Springer, T. A. (1995) *J. Cell Biol.* **128,** 1243–1253
26. Johnston, B., Issekutz, T. B., and Kubes, P. (1996) *J. Exp. Med.* **183,** 1995–2006
27. Berlin, C., Bargatze, R. F., Campbell, J. J., von Andrian, U. H., Szabo, M. C., Hasslen, S. R., Nelson, R. D., Berg, E. L., Erlandsen, S. L., and Butcher, E. C. (1995) *Cell* **80,** 413–422
28. Keating, S. M., Clark, K. R., Stefanich, L. D., Arellano, F., Edwards, C. P., Bodary, S. C., Spencer, S. A., Gadek, T. R., Marsters, J. C., Jr., and Beresini, M. H. (2006) *Protein Sci.* **15,** 290–303
29. Gadek, T. R., Burdick, D. J., McDowell, R. S., Stanley, M. S., Marsters, J. C., Jr., Paris, K. J., Oare, D. A., Reynolds, M. E., Ladner, C., Zioncheck, K. A., Lee, W. P., Gribling, P., Dennis, M. S., Skelton, N. J., Tumas, D. B., Clark, K. R., Keating, S. M., Beresini, M. H., Tilley, J. W., Presta, L. G., and Bodary, S. C. (2002) *Science* **295,** 1086–1089
30. Kelly, T. A., Jeanfavre, D. D., McNeil, D. W., Woska, J. R., Jr., Reilly, P. L., Mainolfi, E. A., Kishimoto, K. M., Nabozny, G. H., Zinter, R., Bormann, B. J., and Rothlein, R. (1999) *J. Immunol.* **163,** 5173–5177
31. Chigaev, A., Blenc, A. M., Braaten, J. V., Kumaraswamy, N., Kepley, C. L., Andrews, R. P., Oliver, J. M., Edwards, B. S., Prossnitz, E. R., Larson, R. S., and Sklar, L. A. (2001) *J. Biol. Chem.* **276,** 48670–48678
32. Chigaev, A., Zwartz, G., Graves, S. W., Dwyer, D. C., Tsuji, H., Foutz, T. D., Edwards, B. S., Prossnitz, E. R., Larson, R. S., and Sklar, L. A. (2003) *J. Biol. Chem.* **278,** 38174–38182
33. Kew, R. R., Peng, T., DiMartino, S. J., Madhavan, D., Weinman, S. J., Cheng, D., and Prossnitz, E. R. (1997) *J. Leukoc. Biol.* **61,** 329–337
34. Liggett, S. B. (1989) *Eur. J. Pharmacol.* **163,** 171–174
35. Shayo, C., Davio, C., Brodsky, A., Mladovan, A. G., Legnazzi, B. L., Rivera, E., and Baldi, A. (1997) *Mol. Pharmacol.* **51,** 983–990
36. Booze, R. M., Crisostomo, E. A., and Davis, J. N. (1989) *J. Pharmacol. Exp. Ther.* **249,** 911–920
37. Foreman, J. C., Norris, D. B., Rising, T. J., and Webber, S. E. (1986) *Br. J. Pharmacol.* **87,** 37–44
38. Freer, R. J., Day, A. R., Muthukumaraswamy, N., Pinon, D., Wu, A., Showell, H. J., and Becker, E. L. (1982) *Biochemistry* **21,** 257–263
39. Green, S. A., Cole, G., Jacinto, M., Innis, M., and Liggett, S. B. (1993) *J. Biol. Chem.* **268,** 23116–23121
40. Ueda, H., Siani, M. A., Gong, W., Thompson, D. A., Brown, G. G., and Wang, J. M. (1997) *J. Biol. Chem.* **272,** 24966–24970
41. Ezeamuzie, C. I., and Philips, E. (2000) *Br. J. Pharmacol.* **131,** 482–488
42. Chen, L. L., Whitty, A., Lobb, R. R., Adams, S. P., and Pepinsky, R. B. (1999) *J. Biol. Chem.* **274,** 13167–13175
43. Lin, K., Ateeq, H. S., Hsiung, S. H., Chong, L. T., Zimmerman, C. N., Castro, A., Lee, W. C., Hammond, C. E., Kalkunte, S., Chen, L. L., Pepinsky, R. B., Leone, D. R., Sprague, A. G., Abraham, W. M., Gill, A., Lobb, R. R., and Adams, S. P. (1999) *J. Med. Chem.* **42,** 920–934
44. Zwartz, G., Chigaev, A., Foutz, T., Larson, R. S., Posner, R., and Sklar, L. A. (2004) *Biophys. J.* **86,** 1243–1252
45. Zwartz, G. J., Chigaev, A., Dwyer, D. C., Foutz, T. D., Edwards, B. S., and Sklar, L. A. (2004) *J. Biol. Chem.* **279,** 38277–38286
46. Cabañas, C., and Hogg, N. (1993) *Proc. Natl. Acad. Sci. U.S.A.* **90,** 5838–5842
47. Stanley, P., Bates, P. A., Harvey, J., Bennett, R. I., and Hogg, N. (1994) *EMBO J.* **13,** 1790–1798
48. Stanley, P., and Hogg, N. (1998) *J. Biol. Chem.* **273,** 3358–3362
49. Wang, L. L., Gaigalas, A. K., Abbasi, F., Marti, G. E., Vogt, R. F., and

[4] A. Chigaev and L. A. Sklar, submitted for publication.

Schwartz, A. (2002) *J. Res. Natl. Inst. Stand. Technol.* **107,** 339–353
50. Zhuang, G., Katakura, Y., Omasa, T., Kishimoto, M., and Suga, K. (2001) *J. Biosci. Bioeng.* **92,** 330–336
51. Alonso, J. L., Essafi, M., Xiong, J. P., Stehle, T., and Arnaout, M. A. (2002) *Curr. Biol.* **12,** R340–R342
52. Ley, K., Laudanna, C., Cybulsky, M. I., and Nourshargh, S. (2007) *Nat. Rev. Immunol.* **7,** 678–689
53. Stein, J. V., and Nombela-Arrieta, C. (2005) *Immunology* **116,** 1–12
54. Miller, L. J., Schwarting, R., and Springer, T. A. (1986) *J. Immunol.* **137,** 2891–2900
55. Prossnitz, E. R. (1997) *J. Biol. Chem.* **272,** 15213–15219
56. Dustin, M. L., and Springer, T. A. (1989) *Nature* **341,** 619–624
57. van der Goot, H., and Timmerman, H. (2000) *Eur. J. Med. Chem.* **35,** 5–20
58. Zhang, L., Jensen, R. T., and Maton, P. N. (1990) *Am. J. Physiol.* **259,** G436–G442
59. Zimmerman, T., and Blanco, F. J. (2008) *Curr. Pharm. Des* **14,** 2128–2139
60. Last-Barney, K., Davidson, W., Cardozo, M., Frye, L. L., Grygon, C. A., Hopkins, J. L., Jeanfavre, D. D., Pav, S., Qian, C., Stevenson, J. M., Tong, L., Zindell, R., and Kelly, T. A. (2001) *J. Am. Chem. Soc.* **123,** 5643–5650
61. Chigaev, A., Wu, Y., Williams, D. B., Smagley, Y., and Sklar, L. A. (2011) *J. Biol. Chem.* **286,** 5455–5463
62. Larson, R. S., Davis, T., Bologa, C., Semenuk, G., Vijayan, S., Li, Y., Oprea, T., Chigaev, A., Buranda, T., Wagner, C. R., and Sklar, L. A. (2005) *Biochemistry* **44,** 4322–4331
63. Njus, B. H., Chigaev, A., Waller, A., Wlodek, D., Ostopovici-Halip, L., Ursu, O., Wang, W., Oprea, T. I., Bologa, C. G., and Sklar, L. A. (2009) *Assay. Drug Dev. Technol.* **7,** 507–515
64. Sarantos, M. R., Raychaudhuri, S., Lum, A. F., Staunton, D. E., and Simon, S. I. (2005) *J. Biol. Chem.* **280,** 28290–28298
65. Takada, Y., Ye, X., and Simon, S. (2007) *Genome Biol.* **8,** 215
66. Huhtala, M., Heino, J., Casciari, D., de Luise, A., and Johnson, M. S. (2005) *Matrix Biol.* **24,** 83–95
67. Shamri, R., Grabovsky, V., Gauguet, J. M., Feigelson, S., Manevich, E., Kolanus, W., Robinson, M. K., Staunton, D. E., von Andrian, U. H., and Alon, R. (2005) *Nat. Immunol.* **6,** 497–506
68. Salas, A., Shimaoka, M., Kogan, A. N., Harwood, C., von Andrian, U. H., and Springer, T. A. (2004) *Immunity* **20,** 393–406
69. Eniola, A. O., Krasik, E. F., Smith, L. A., Song, G., and Hammer, D. A. (2005) *Biophys. J.* **89,** 3577–3588
70. Shimaoka, M., and Springer, T. A. (2004) *Curr. Top. Med. Chem.* **4,** 1485–1495
71. Laudanna, C. (2005) *Nat. Immunol.* **6,** 429–430
72. Woska, J. R., Jr., Shih, D., Taqueti, V. R., Hogg, N., Kelly, T. A., and Kishimoto, T. K. (2001) *J. Leukoc. Biol.* **70,** 329–334
73. Thelen, M., and Stein, J. V. (2008) *Nat. Immunol.* **9,** 953–959
74. Alon, R., and Shulman, Z. (2011) *Exp. Cell Res.* **317,** 632–641
75. Benschop, R. J., Nijkamp, F. P., Ballieux, R. E., and Heijnen, C. J. (1994) *Br. J. Pharmacol.* **113,** 1311–1316
76. Benschop, R. J., Rodriguez-Feuerhahn, M., and Schedlowski, M. (1996) *Brain Behav. Immun.* **10,** 77–91
77. Schedlowski, M., Hosch, W., Oberbeck, R., Benschop, R. J., Jacobs, R., Raab, H. R., and Schmidt, R. E. (1996) *J. Immunol.* **156,** 93–99
78. Dimitrov, S., Benedict, C., Heutling, D., Westermann, J., Born, J., and Lange, T. (2009) *Blood* **113,** 5134–5143
79. Dimitrov, S., Lange, T., and Born, J. (2010) *J. Immunol.* **184,** 503–511
80. Prossnitz, E. R., and Ye, R. D. (1997) *Pharmacol. Ther.* **74,** 73–102
81. Maestes, D. C., Potter, R. M., and Prossnitz, E. R. (1999) *J. Biol. Chem.* **274,** 29791–29795